International Journal of Computational Vision and Biomechanics
Vol. 5 No. 1 (January-June, 2019)

MUK PUBLICATIONS
Open Access Publisher

Parametric Geometrical Subject-specific Finite Element Models of the Proximal Femur: A Tool to Predict Slipped Capital Femoral Epiphyses

O. Paseta[a], M. J. Gómez-Benito[a], J.M. García-Aznar[a], C. Barrios[b], M. Doblaré[a].

[a]*Group of Structural Mechanics and Materials Modelling, Aragon Institute of Engineering Research (13A) University of Zaragoza, María de Luna s/n, 50018, Zaragoza, Spain*
[b]*Orthopaedics and Trauma Unit, Department of Surgery, Valencia University Medical School, Valencia, Spain*

Submitted: 10th September 2018 ***Revised: 25th November 2018*** ***Accepted: 05th January 2019***

*Different anatomical and mechanical factors inducing growth plate overloading have been implicated in the etiology of Slipped Capital Femoral Epiphysis (SCFE). Loading and the subsequent risk of fracture at the epiphyseal growth plate of the femoral head have been poorly investigated so far, so in this work, we analyse Slipped Capital Femoral Epiphysis from a mechanical point of view. The aim of this research is to determine the influence of the proximal femoral geometry on the growth plate slippage. This is accomplished by means of Finite Element Analyses (FEA) of a parametric model of the proximal femur previously created. An adolescent standardized femur is defined based on average geometrical parameters collected in literature of healthy and slipped hips. In order to evaluate the potential of this parametric model, we compared successfully their results with those obtained using models from actual geometries of a pre-SCFE and a healthy hip of a child. Next, this parametric model is adapted to simulate subject specific situations. The most important parameters: the Physis Sloping Angle (*PSA*) and the Posterior Sloping Angle of the Physis (*L*), are varied and their effect under the same loads corresponding to walking and stairs climbing is investigated. The computed results show a strong dependence of the growth plate failure on the geometry of the proximal femur. Higher values of the Physis Sloping Angle (*PSA*) and the Posterior Sloping Angle (*L*) are related to higher growth plate stresses and therefore to a more likely slippage. The highest stress level is always found in the medial region of the physis, a site where usually growth plate starts to fail.*

Key words: *Slipped Capital Femoral Epiphysis, Finite Element Analysis, Growth Plate, Biomechanical Parametric Model.*

1. INTRODUCTION

Slipped Capital Femoral Epiphysis (SCFE) is the most common disorder of the adolescent hip [1]. It occurs in 5 of 100.000 children from 10 to 15 years old [2,3]. SCFE consists on a posterior and medial slippage of the proximal femoral epiphysis at the metaphysis, occurring through the physeal plate. The diagnosis of SCFE is, unfortunately, not easy in many cases which implies a delay in its treatment. This delay results in a less favorable long-term prognosis [1] and risk of other secondary effects, such as, osteonecrosis of the femoral head [4] and degenerative hip arthritis [1]. Thus, it is very important to develop predictive methods for early detection of SCFE.

Different factors such as endocrine disorders [5] and radiation therapy [6] have been found to be associated with the development of SCFE. However, in most cases the aetiology remains unknown. Idiopathic SCFE has been related to many factors, including overweight [7], physeal orientation [8,9], abnormalities in the physeal architecture [10,11] and hormonal changes during adolescence that affect the physeal strength [1].

The stress magnitude at the femoral capital physis under physiological and overweight loads has not been sufficiently addressed. To our knowledge, the analysis of the different factors affecting SCFE have been mainly focused on several geometrical features of the proximal femur and parameters such as weight, height or age of the patient [8,9]. However, mechanical factors, such as strain and stress distributions on the growth plate, which could explain failure of the proximal growth plate have not been fully studied. A recent work of Fishkin *et al.* [12] analyzed the stress distribution in the growth plate in the stance phase activity varying the angle of the femoral neck version. We also recently presented a finite element model of both proximal femora of a child affected by pre-SCFE in his left leg and compared the distribution of stresses in both growth plates when performing different activities [13]. However, a wider study is needed to determine the stress distributions at the proximal femur physeal plate on different patients. Indeed, the determination of the stress level in the growth plate could help to estimate the subjects with a higher probability of slippage.

When a Finite Element model is developed, segmentation of the proximal femur and generation of the associated FE mesh are the most time consuming parts of the process. In this work, we propose the use of a parametric model, where the proximal femur geometry is simplified and defined through a set of anatomical parameters: Neck-Diaphysis Angle, Neck Shaft Plate Shaft Angle, Head radius, Medullary channel width; which can be easily adapted to each specific subject. This simplified geometry can be meshed by means of automatic mesh generation

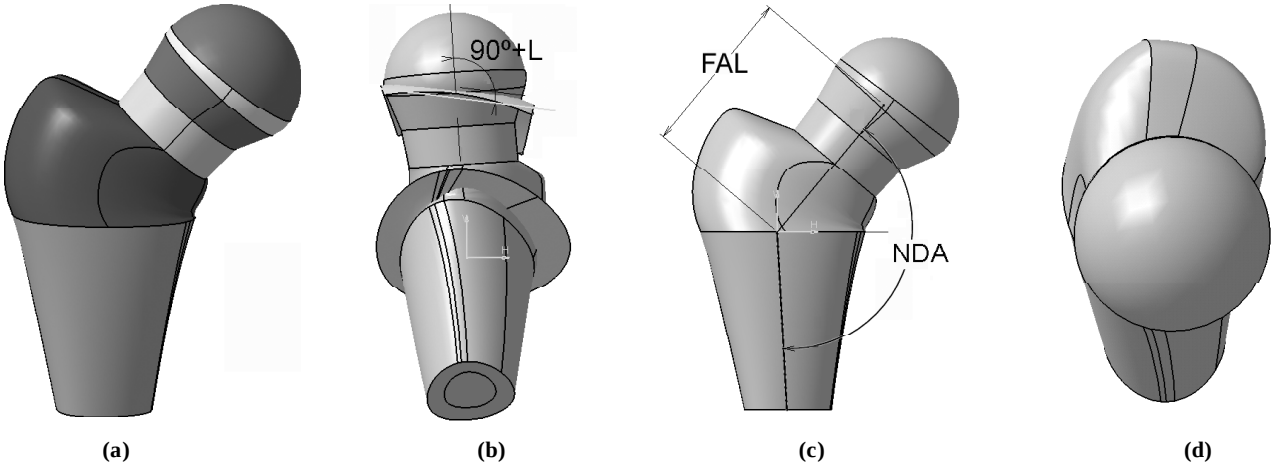

Figure 1: Parametrized geometry of the proximal femur (a) different primitive geometries; (b) lateral view; (c) anterior-posterior view; (d) upper view.

programs with good finite element aspect ratios for all the mesh. This model can help to determine the risk of development of SCFE, based on the geometrical morphology of each specific patient's hip. Therefore, the aim of this paper is to develop a model for the parametrized geometry of the proximal femur and evaluate differences in the stress distribution that appears in the growth plate for different femoral configurations.

2. MATERIAL AND METHODS

A parametric geometry of the proximal femur including epiphyseal growth plate was developed, based on several parameters that determine the geometry of the proximal femur: head radius (*HR*), physeal width (*PW*), neck shaft-neck plate angle (*NSNPA*), posterior slopping angle (*L*), physis-diaphysis angle (*PDA*), cortical thickness (*CT*), femoral neck width (*FNW*), diaphyseal width (*DW*) (Figs. 1 and 3). These parameters can be trivially modified to simulate different femurs and plates, being therefore easily to adapt to each specific subject.

To develop this parametric model we initially reconstructed the geometry of both proximal femora of a 14-year-old boy with pre-SCFE in his left hip from a set of CT-scans. The geometry of these femurs and epiphyseal plates were simplified by means of primitive geometries (Fig. 1.a) and reconstructed through the CAD-program Catia [14]. Then, it was automatically meshed by Harpoon [15] (Fig. 4) with hexahedral elements of characteristic length of 3mm. The geometry of this parametric model can be easily resized and modified to simulate different geometries, a scheme of the process followed to simulate the different geometries and the time consumed in each step could be observed in figure 2.

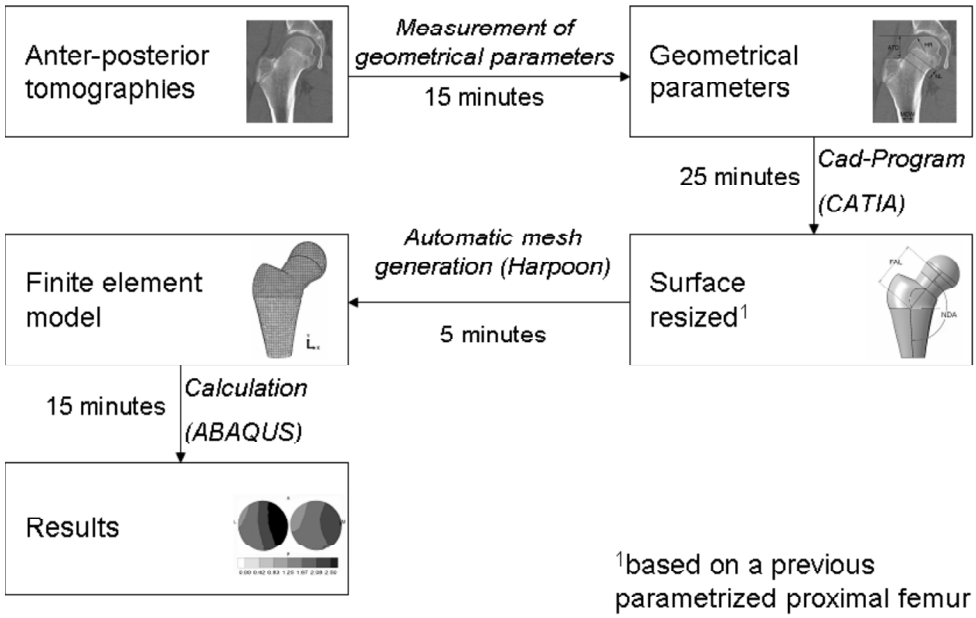

Figure 2: Scheme of the process to obtain the specific subject finite element model including the approximate time consumed in each step.

In order to address the main aim of this paper, three different analyses were performed. First, we evaluated the accuracy of the parametric model. Hence, we developed four finite element models, two of them based on the actual geometry of the two femurs of a 14-year-old boy with pre-SCFE in his left hip and body weight of 92kg, whereas the other two were based on the parametrized geometry of these same femurs. In the second set of analyses, we created two additional independent parametrised models to determine the influence of the overall geometry into the growth plate slippage. The parametrised geometry of these femurs was based on measurements of morphometric parameters of a previous study of 36 healthy hips and 47 unaffected hips of patients with unilateral SCFE [8]. The mean values of these parameters were used to reconstruct the parametrised geometry of a healthy "standardised" femur and a "standardised" nonslipped hip of children with unilateral SCFE. This second femur has been reported to be more prone to suffer slippage [8]. The body weight for both "standardised" femurs was estimated in 58.8kg [8] in order to minimize the influence of the body weight on the results. Finally, we performed a sensitivity analysis with respect to different geometrical parameters that are the most determinant in the development of SCFE [8] in order to determine their respective individual influence: the physeal slopping angle (*PSA*) and the posterior slopping angle (*L*) were varied in ten degrees in two independent models based on the geometry of the "standardised" healthy femur.

The geometrical parameters which define the geometry of the simulated femurs are summarized in table 1. In all cases, the growth plate thickness was assumed constant and estimated in 1mm [16]. We considered three different materials: cartilage for the growth plate, trabecular and cortical bone. Linear elastic isotropic behavior was assumed for all of them with elastic moduli of 5MPa, 700MPa and 17000MPa and Poisson's ratios of 0.45, 0.2 and 0.3 respectively [17,18,19]. Different loading conditions were simulated in each analysis: (1) heel strike during walking; (2) midstance; (3) toe off; (4) heel strike during stairs climbing. These loads were applied on the femoral head including also the reaction at the abductor. Both were scaled by the body weight of the patient (Table 2)[20].

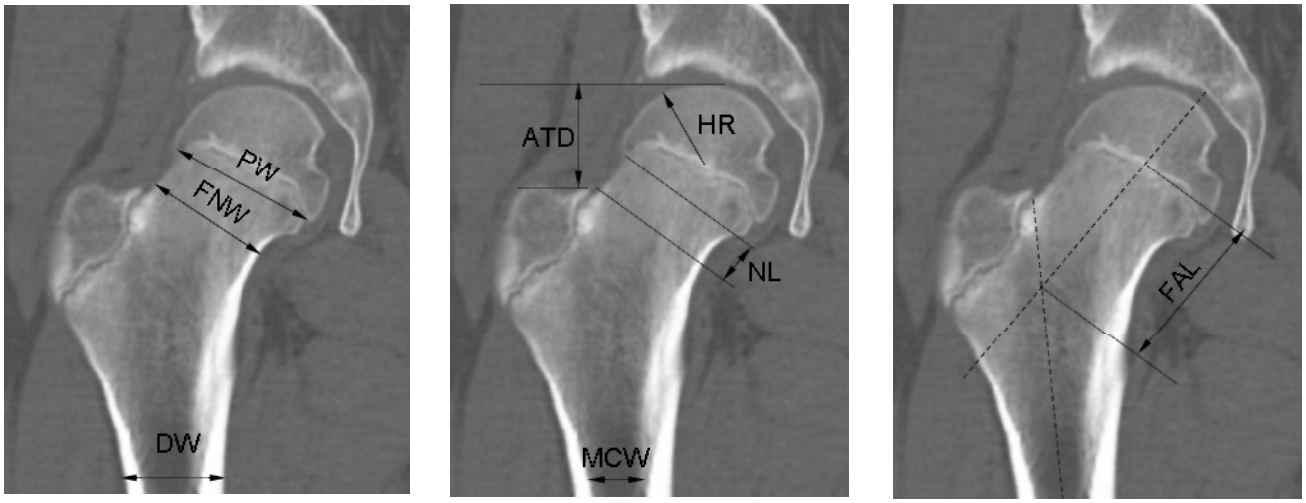

Figure 3: Geometrical parameters of the defined femurs measured on anterior-posterior tomographies (acronyms are fully defined in table 1)

Growth plate failure is assumed to be mainly produced by a combination of shear stresses, which may induce slip of the head, and tensile stresses, that might tear up the growth plate from the trabecular bone [10,11,21,22,23]. In order to estimate the growth plate risk to failure, we chose the Tresca failure criterion because it is the most appropriate for shear failure. We could also consider von Misses stresses which takes into account normal and shear stresses. In fact, von Misses stress for the analysed load cases were qualitatively similar to Tresca's although the latter resulted slightly lower, the conclusions drawn from von Misses stress distributions were the same than those obtained from Tresca stresses [13].

3. RESULTS

First, the distributions of Tresca stresses and the maximum value of these stresses at the growth plate were compared between the models developed for actual and parametric geometries of these femurs. Second, we analysed the stress distribution on the two standardised healthy and affected femurs. Finally, the stress distribution was studied for the standardised healthy femur after modifying the posterior slopping angle (PSA) in 10º and the physeal slopping angle (L) also in 10º.

3.1 Comparative validation of the parametric model

To evaluate the parametric model, the results obtained in a FE analysis of real geometry were compared to those computed from the parametrised geometry. The Tresca stress distributions for the different activities simulated at the growth plate are shown from an upper view in figure 5. The load transfer mechanism through the growth plate in both models was very similar. A stress concentration at the medial

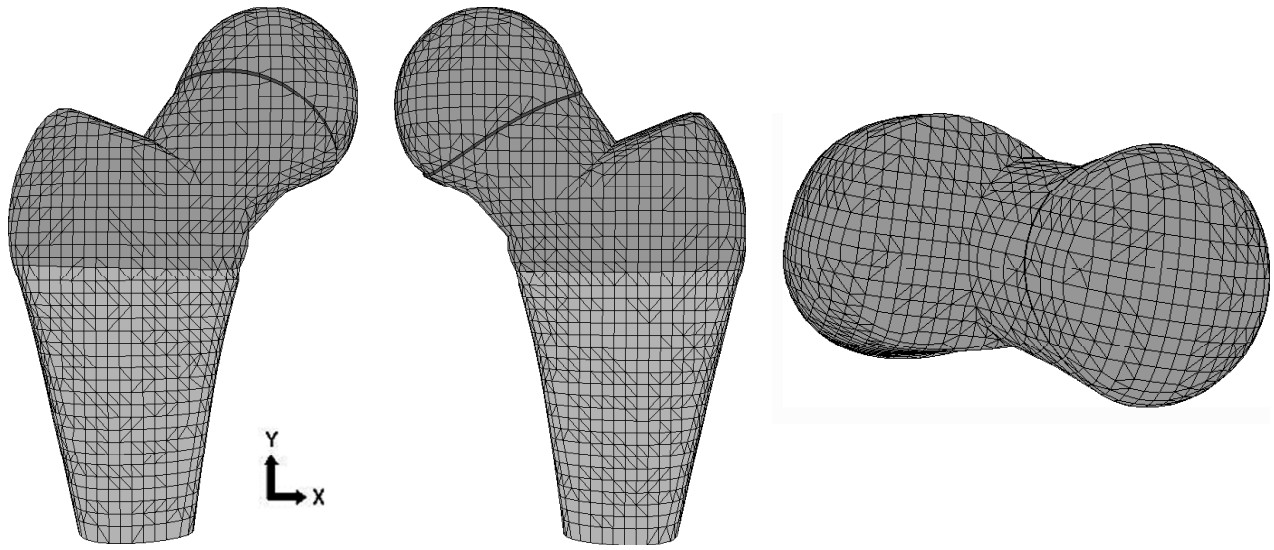

Figure 4: Finite element model of the healthy femur including the growth plate based on the parametrised geometry.

Table 1
Geometrical Parameters of the Simulated Femurs [8,13].

	Patient		*"Standardised" [8]*		*Sensitivity analysis*	
Geometric Parameters	*Healthy*	*pre-SCFE*	*Healthy*	*Affected*	*L angle*	*PSA*
Growth Plate Area (cm^2)	30,9	24,7	15.2	14.5	15.2	15.2
Neck-Diaphysis Angle (NDA) (o)	48	51	39.2	39.2	39.2	39.2
Neck Shaft Plate Shaft (NSPSA) (o)	18	14	8.1	4.6	8.1	1.7
Posterior Sloping Angle of Physis (L) (o)	11	13	5.0	13.6	**15.0**	5.0
Physeal slopping angle (PSA) (o)	26	34	30	34	30	**40**
Physeal diaphysis angle (PDA) (o)	59	55	59	55	59	49
Head radius (HR) (mm)	32.4	33	22	21.5	22	22
Femoral neck width (FNW) (mm)	26	24	17.5	17	17.5	17.5
Medullary channel width (MCW) (mm)	25	24	15	15	15	15
Diaphyseal width (DW) (mm)	40	40	28	28	28	28
Femoral axis length (FAL) (mm)	78	77	56	56	56	56
Articulo trochanteric distance (ATD) (mm)	35	33	25	23	25	25
Plate thickness (PT) (mm)	1	1	1	1	1	1
Neck length (NL) (mm)	18	20	14	14	14	14
Diaphyseal length (DL) (mm)	84	81	58.75	58.75	58.75	58.75

Table 2
Components of the Femoral Loads for each Activity Simulated, Normalized to the Body Weight (BW) [20].
Reference Axes in Figure 4

	Head Load (N)			*Abductor Load (N)*		
Load case	*X Dir.*	*Y Dir.*	*Z Dir.*	*X Dir.*	*Y Dir.*	*Z Dir.*
Heel strike during walking	-0.32·BW	-2.21·BW	-2.95·BW	0.78·BW	0.76·BW	0.14·BW
Midstance	0.74·BW	-0.86·BW	-0.41·BW	-0.34·BW	0.05·BW	0.02·BW
Toe off	-0.36·BW	-0.59·BW	1.31·BW	0.21·BW	0.44·BW	-0.13·BW
Heel strike during climbing stairs	-0.41·BW	-2.27·BW	-0.70·BW	0.89·BW	1.00·BW	0.32·BW

area was observed at the heel strike moment during stairs climbing; this concentration was also medial in the pre-slipped hip, but oriented towards the anterior area in both parametric and real geometries at this pre-slipped hip. In addition, the maximum Tresca stresses were always higher for the pre-slipped hip when compared to the healthy model in both actual and parametrised geometries.

3.2 Standardised Femurs

The parametrised geometry of the femur was adapted to the geometry of a "standardised" healthy femur and a "standardised" non-affected hip of children with unilateral SFCE. The healthy growth plate of the SCFE-affected child exhibited higher stresses (Fig. 6) than the growth plate of the healthy femur used as control. During heel strike, while

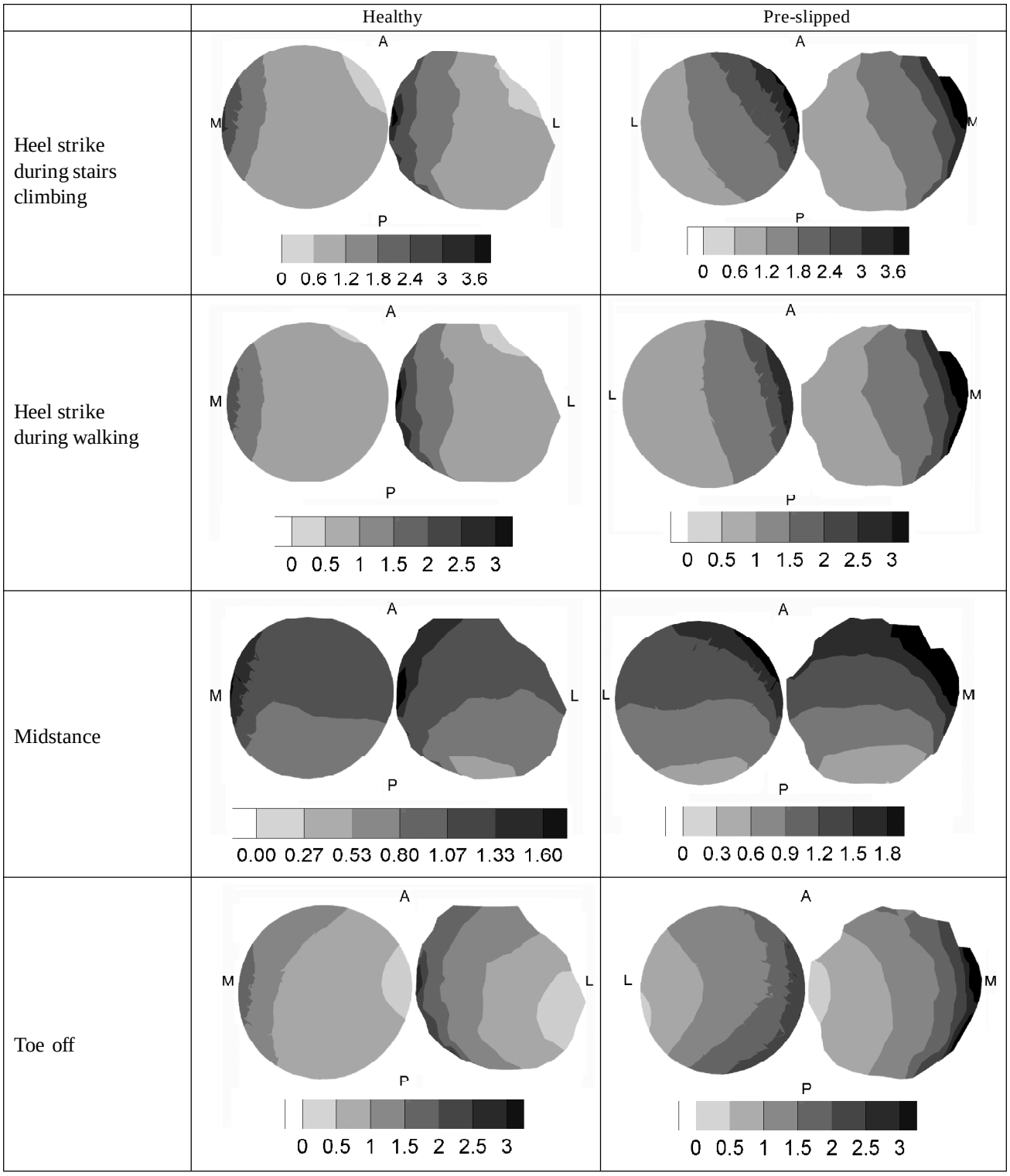

Figure 5: Distributions of Tresca stresses (MPa) at the plates of a 14 year old child, models based on parametrised and real geometry (A-Anterior, P-Posterior, M-Medial, L-Lateral).

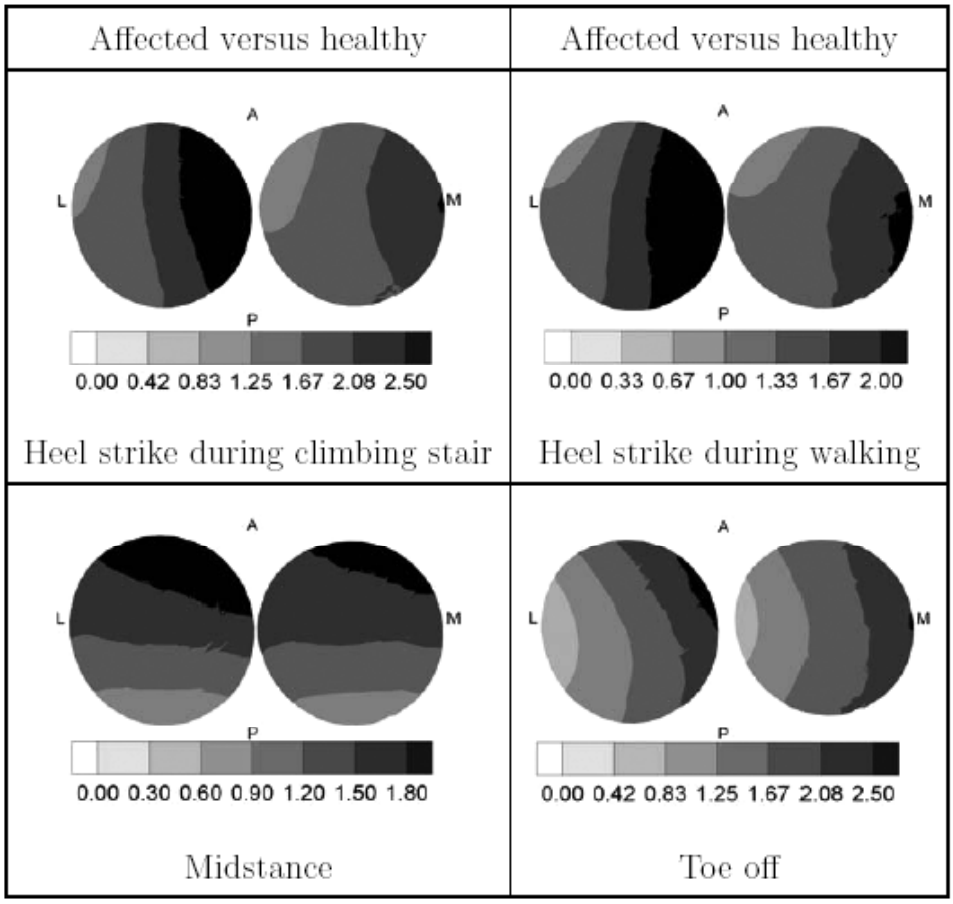

Figure 6: Distributions of Tresca stresses (MPa) at the parametrised growth plates of the "standardised" affected and "standardised" healthy femurs (A-Anterior, P–Posterior, M-Medial, L-Lateral).

stairs climbing, Tresca stresses over 2.5MPa were observed at the medial region of the affected growth plate. A stress concentration was also observed in this same region of the healthy hip, although with a lower value of the Tresca stress. No area appeared with stresses higher than 2.5MPa the difference was not so apparent at midstance and toe off, but the stresses were always higher for the affected hip than for the healthy one. At the midstance stage, the stress concentration was localized in the anterior region of the physis.

3.3 Influence of the Posterior Slopping Angle and the Physeal Slopping Angle

Tresca stresses increased with both angles: posterior slopping and physeal slopping. The greatest differences were observed when increasing the physeal slopping angle (Fig. 7). At the heel strike stage, during stairs climbing, a maximum Tresca stress of 2.15MPa for the standardised healthy growth plate was observed. This stress increased to values higher than 2.5MPa when increasing the L angle in 10º and the PSA in 10º (Fig. 7), being the area subjected to this stress bigger when increasing the PSA. The maximum Tresca stresses were localized in the medial region during heel strike and toe off, while this concentration appeared in the anterior region during the midstance phase.

4. DISCUSSION

This paper describes how a parametrised geometry of the proximal femur morphology of a child may be used to fastly obtain a prediction of the stress distribution at the growth plate and thus determine the risk of development of SCFE. Despite the qualitative character of the conclusions here obtained, the proposed model might be useful to determine if pinnig of the healthy femur can be recommended or not in patients suffering from unilateral SCFE.

To evaluate the potential of this parametrised model we performed a comparison between the results obtained by means of finite element simulations of actual geometries of the proximal femurs of a child and the parametrised geometry of these same femurs. The similar distributions of stresses computed in both growth plates validate the accuracy of the parametric finite element model. Even though the distributions were not identical, the parametrised model was able to identify the areas of maximum stresses and the maximum value of the Tresca stress with sufficient accuracy.

Assuming the same body weight, the differences observed between the standardised healthy femur and the parametrised unaffected femur of children with unilateral SCFE, indicate the strong influence of the geometrical parameters on the development of slipped capital ephiphisis [8, 9, 24]. The differences in stresses when modifying the L

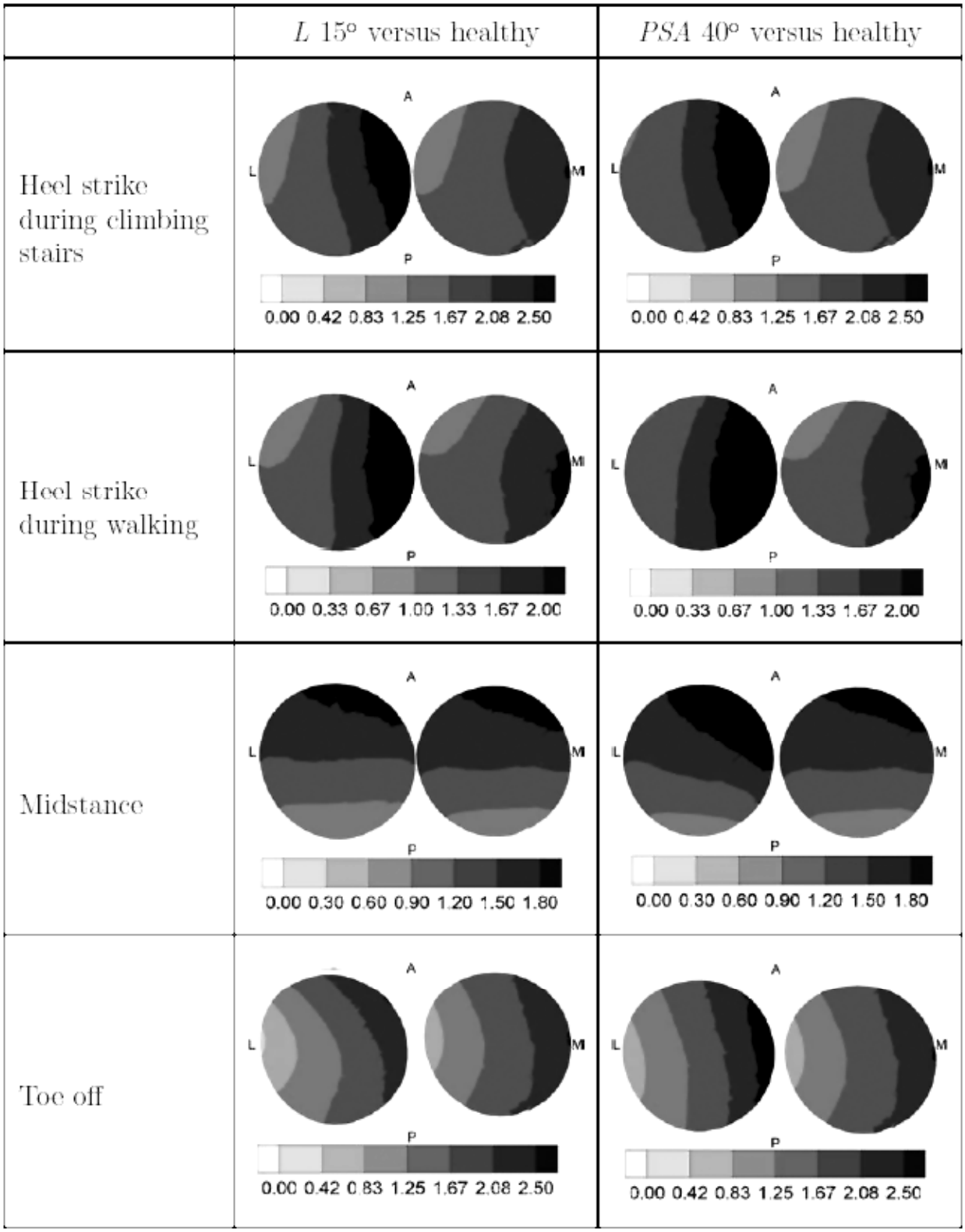

Figure 7: Distributions of Tresca stresses (MPa) at the parametrised growth plates of the standardised healthy femur when varying the L angle and PSA in 10° (A-Anterior, P-Posterior, M-Medial, L-Lateral).

and PSA angles follow a similar trend to that observed clinically [9,8]. Highest values of L and PSA angles resulted in higher stresses and therefore a higher probability of slippage. However, the same variation in L and PSA angle results in a different influence on the stress distribution. When modifying the L angle in 10º an increase of 15% was observed in the maximum Tresca stress at the heel strike moment during stairs climbing and walking. These

differences were higher when increasing the PSA angle: an increase of the Tresca stress of about 35% was observed at the moment of heel strike.

The highest stress concentration was observed at the medial region of the physis at the heel strike moment during stairs climbing. Worse mechanical properties have been reported at the posterior-medial area of the physis [25]. These two facts could indicate the beginning of the plate failure in the medial region.

Despite the results obtained, we have to keep in mind that modelling in biomechanics involves a number of simplifications on different levels that have to be interpreted carefully. The main assumptions of this work are:

First, we assume all materials to be linear elastic. This hypothesis has been used by many authors in FE models of bone and cartilage [26] reporting sufficiently accurate results for this type of analyses. The mechanical properties used for the growth plate were determined from animal experiments [10,11]. We have to remark the few experimental works designed to obtain mechanical properties of femoral growth plates [21]. There are several works to determine the mechanical properties in bovine tibial growth plates. Ultimate shear stress was reported to be between 1.66MPa and 3.81MPa depending on the anatomical location [11] and tensile stress between 0.83MPa and 1.89MPa [10]. In bovine distal femora the maximum and average ultimate tensile stress registered were 5MPa and 3MPa respectively [25]. The differences reported may be due to biologic variations, animal specie, anatomic form of the growth plate and testing modalities. To our knowledge, there are very few experimental works performed to determine mechanical properties of human growth plates, thus the properties had to be extracted from animal experiments and our results has to be analysed from a qualitative point of view. The same elastic moduli and Poisson's ratios were considered for the simulated hips despite the fact that these properties decrease in slipped hips [27].

Second, the applied forces used to drive the simulations were considered the same (just scaled by the body weight) for healthy, pre-slipped and unaffected hips of children affected by unilateral SCFE, although they are likely to vary between normal and diseased children due to compensatory mechanisms [27].

Third, other effects such as the influence of cyclic loads that could produce fatigue and a possible increment of cartilage stiffness due to closing of cartilage pores by plate compression have not been considered in this approach. As has been reported in a previous work [13], we do not take into consideration the poroelastic behavior of the growth plate because the same conclusions as in the elastic model may be drawn.

Finally, the growth plate was considered homogeneous not taking into account its microstructural properties which may vary with age and sex. The microstructural geometry and mechanical properties of the physis could influence the failure mechanism locally [28]; however we are most interested in the global failure mechanism. Few experimental works have been performed to determine the mechanism of failure of the growth plate. Moen and Pelker [28] tested bovine femurs and tibias to determine the failure mechanism of the growth plate. They concluded that a different mechanism and zone of failure is expected when loading the specimens in tension, shear or compression. For each of these load cases, failure is expected in the hypertrophic zone, columnation zone and ossification zone respectively. Also the loading rate, maturity of the physis and sex alter the zones and mechanism of failure. All these effects have not been taken into consideration in this work.

The uncertainties in data of mechanical properties, correct consideration of loading, material characterization and geometric modelling are a direct consequence of the fact that each individual is unique. Average values might not be representative of a large percentage of the cases of interest. Therefore a more flexible and easily adjustable model to make approximate subject-specific analyses could be helpful when studying each specific individual. The parametrised geometry of the proximal femur in combination with FE is, despite the simplifications made in the geometry, suitable for the assessment of magnitudes of stress under mechanical loads for subject-specific geometries, so it can be used to determine the risk of SCFE development in different individuals, and help to a very important early diagnosis and a successful outcome [29].

ACKNOWLEDGMENTS

The authors gratefully acknowledge the research support of the Spanish Ministry of Science and Technology through the research project DPI2006-09692 and the finantial support by IBERCAJA.

REFERENCES

[1] R. T. Loder, Slipped capital femoral epiphysis, *Am Fam Physician* 57(9) (1998) 2135-42.

[2] S. T. Canale, Campbell's Operative Orthopaedics, 2003, pp. 1481-1503.

[3] R. T. Loder, The demographics of slipped capital femoral epiphysis. an international multicenter study., Clin Orthop Relat Res. 322 (1996) 8-27.

[4] J. G. Kennedy, M. T. Hresko, J. R. Kasser, K. B. Shrock, D. Zurakowski, P. M. Waters, M. B. Millis, Osteonecrosis of the femoral head associated with slipped capital femoral epiphysis, J Pediatr Orthop 21(2) (2001) 189-193.

[5] R. T. Loder, B. Wittenberg, G. DeSilva, Slipped capital femoral epiphysis associated with endocrine disorders, J Pediatr Orthop 15(3) (1995) 349-356.

[6] R. T. Loder, R. N. Hensinger, P. D. Alburger, D. D. Aronsson, J. H. Beaty, D. R. Roy, R. P. Stanton, R. Turker, Slipped capital femoral epiphysis associated with radiation therapy, J Pediatr Orthop 18(5) (1998) 630-636.

[7] E. M. Manoff, M. B. Banffy, J. J. Winell, Relationship between body mass index and slipped capital femoral epiphysis, J. Pediatr Orthop 25(6) (2005) 744-746.

[8] C. Barrios, M. A. Blasco, M. C. Blasco, J. Gascó, Posterior sloping angle of the capital femoral physis. a predictor of

bilatery in slipped capital femoral epiphysis., *J. Pediatr. Orthop*. 25(4) (2005) 1067-1078.

[9] J. W. Pritchett, K. D. Perdue, G. Dona, The neck shaft-plate shaft angle in slipped capital femoral epiphysis, *Orthop. Rev.* 18(11) (1989) 1187-1192.

[10] J. L. Williams, P. D. Do, J. D. Eick, T. L. Schmidt, Tensile properties of the physis vary with anatomic location, thickness, strain rate and age, *J. Orthop. Res*. 19 (2001) 1043-1048.

[11] J. L. Williams, J. N. Vani, J. D. Eick, E. C. Petersen, T. L. Schmidt, Shear strength of th physis varies with anatomic location and is a function of modulus, inclination and thickness, *J. Orthop. Res*. 17 (1999) 214-222.

[12] Z. Fishkin, D. G. Armstrong, H. Shah, A. Patra, W. M. Mihalko, Proximal femoral physis shear in slipped capital femoral epiphysis-a finite element study, *J. Pediatr. Orthop*. 26(3) (2006) 291-294.

[13] O. Paseta, M. J. Gómez-Benito, J. M. García-Aznar, C. Barrios, J. Gascó, M. Doblaré, Biomechanical analysis of a slipped capital femoral epiphysis, Medical Engineering and Physics (submitted).

[14] CATIA, Version 5, release 11 online documentation, dassaut systems, 1994-2003.

[15] Harpoon, Version 2.0, cei.

[16] D. D. Cody, G. J. Gross, F. J. Hou, H. J. Spencer, S. A. Goldstein, D. P. Pyhrie, Femoral strength is better predicted by finite element models than QCT and DXA, *J. Biomech*. 32 (1999) 1013-1020.

[17] W. C. Hayes, J. L. W. Swenson, D. J. Schurman, Asymmetrix finite element analysis of the lateral tibial plateau, *J. Biomech*. 11 (1978) 21-33.

[18] F. G. Evans, Mechanical Properties of Bone, Charles C. Thomas, 1973.

[19] R. L. Spilker, J. K. Suh, V. C. Mow, A finite element analysis of the indentation stress-relaxation response of linear biphasic articular cartilage., *J. Biomech Eng*. 114(2) (1992) 191-201.

[20] V. M. Goldberg, D. T. Davy, G. L. Kotzar, *et al*., In Vivo Hip Forces, New York, 1988, pp. 251-255.

[21] S. M. Chung, S. C. Batterman, C. T. Brighton, Shear strength of the human femoral capital epiphyseal plate, *J. Bone Joint Surg. Am*. 58(1) (1976) 94-103.

[22] J. W. Pritchett, K. D. Perdue, Mechanical factors in slipped capital femoral epiphysis, *J. Pediatr. Orthop*. 3 (1989) 385-388.

[23] H. M. Litchman, J. Duffy, Slipped capital femoral epiphysis: Factors shear forces on the epiphyseal plate, *J. Pediatr. Orthop*. 4 (1984) 745-748.

[24] J. Kordelle, M. Millis, F. A. Jolesz, R. Kikinis, J. A. Richolt, Three-dimensional analysis of the proximal femur in patients with slipped capital femoral epiphysis based on computed tomography, *J. Pediatr. Orthop*. 21(2) (2001) 179-182.

[25] B. Cohen, G. S. Chorney, D. P. Phillips, H. M. Dick, J. A. Buckwalter, A. Ratcliffe, V. C. Mow, The microstructural tensile properties and biochemical composition of the bovine distal femoral growth plate, *J. Orthop. Res*. 10(2) (1992) 263-275.

[26] S. Kumaresan, N. Yoganandan, F. A. Pintar, D. J. Maiman, Biomechanical study of pediatric human cervical spine: A finite element approach, *J. Biomech. Eng*. 122(1) (2000) 60-71.

[27] K. M. Song, S. Halliday, C. Reilly, W. Keezel, Gait abnormalities following slipped capital femoral epiphysis. 24(2) (2004) 148-155.

[28] C. T. Moen, R. R. Pelker, Biomechanical and histological correlations in growth plate failure, *J. Pediatr. Orthop*. 4(2) (1984) 180-184.

[29] T. Odent, S. Pannier, C. Glorion, Epifisiólisis femoral superior, Enciclopedia médico-quirúrjica 14 (2006) 396-401.